The ATLAS Electron and Photon Triggers

Samuel David Jones, on behalf of the ATLAS Collaboration

School of Mathematical and Physical Sciences, Pevensey II, University of Sussex, Falmer Campus, Brighton, BN1 9QH, United Kingdom

E-mail: samuel.david.jones@cern.ch

Abstract. Electron and photon triggers covering transverse energies from 5 GeV to several TeV are essential for signal selection in a wide variety of ATLAS physics analyses to study Standard Model processes and to search for new phenomena. The ATLAS trigger system is divided in a hardware-based Level-1 trigger and a software-based high-level trigger, both of which were upgraded during the LHC shutdown in preparation for Run 2 operation. To cope with the increasing luminosity and more challenging pile-up conditions at a centre-of-mass energy of 13 TeV, the trigger selections at each level are optimised to control the rates and keep efficiencies high. To achieve this goal multivariate analysis techniques are used. The ATLAS electron and photon triggers and their performance with Run 2 data are presented.

1. Introduction

The ATLAS [1] electron and photon (e/γ) triggers select events with electrons and photons from the huge amount of data produced by high energy proton-proton collisions at the Large Hadron Collider [2], only a fraction of which can be recorded. Electrons and photons are common to many interesting experimental signatures at the LHC. For example, $W \to e\nu$ was a key channel for the measurement of the W mass [3] and photon signatures played a major role in the Higgs boson discovery [4]. Electrons and photons are also present in many new physics scenarios.

In Run 2, the LHC has reached a peak instantaneous luminosity of 16.8×10^{33} cm^{2}s^{-1}, twice the level seen during Run 1. The increased rate of collision data offers enormous physics potential, presenting new challenges for the e/γ triggers in the form of increased rates and harsher pileup conditions. Many improvements have been made in Run 2 to the e/γ triggers to maintain efficiencies at Run 1 levels for as long as possible whilst keeping the rates at a manageable level.

These proceedings provide a brief overview of the design and recent upgrades to the ATLAS e/γ triggers as well their performance in 2016 and 2017 data taking.

2. The ATLAS Electron and Photon Triggers

e/γ triggers at ATLAS select events based on inputs from the calorimeter and the inner detector. The calorimeter system measures the energy deposits with an outer hadronic layer and an inner electromagnetic layer. These surround the inner detector, which provides the tracking of charged particles with a pixel detector and semiconductor tracker. A Transition Radiation Tracker (TRT) allows for additional separation of electrons and photons and adds particle identification capability based on transition radiation.

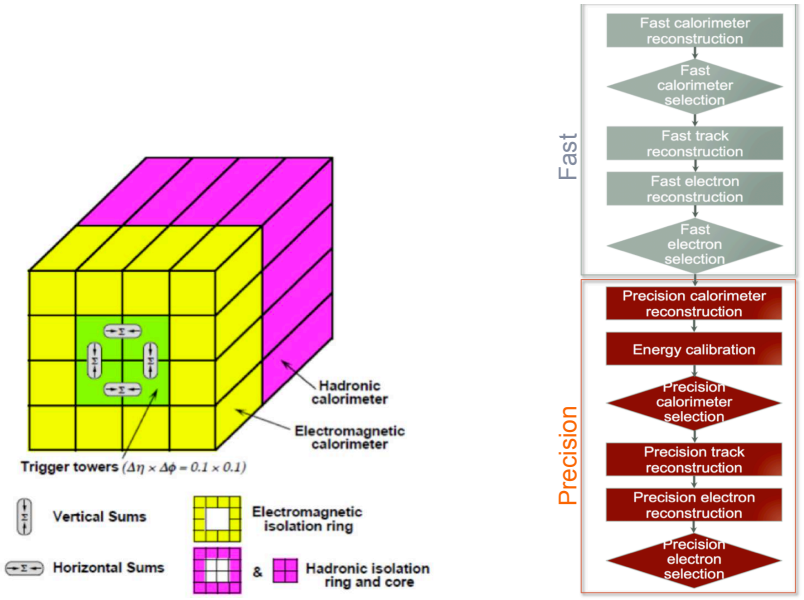

Figure 1. Schematic of the L1 calorimeter step (left) and the HLT trigger algorithm (right). At L1 a sliding-window algorithm uses the four overlapping trigger towers highlighted in green to locate a local energy maximum for energy reconstruction. The HLT process consists of a fast sequence for early rejection which precedes more precise offline algorithms for the final selection.

The ATLAS trigger system uses these inputs to provide a trigger "decision" on whether events are recorded, reducing the rate from 40 MHz to $\sim$ 1 kHz, around 20% of which is reserved for e/γ triggers. The e/γ trigger decision begins at Level 1 (L1) which identifies Regions-Of-Interest (ROIs) based on hardware information. The High Level Trigger (HLT) is then seeded by the ROI, using the full detector granularity in this region to provide the final trigger decision.

The L1 trigger decision uses calorimeter information to build an ROI consisting of 4×4 trigger towers (see figure 1), analogue summations of energy in the calorimeter cells, with granularity 0.1×0.1 in pseudorapidity (η) and azimuthal angle (ϕ). A transverse energy (E_{T}) threshold is applied, which is η dependent to account for energy losses and the geometry of the detector. A sliding-window algorithm identifies a local energy maximum using four overlapping towers within a 2×2 central region for EM energy reconstruction. The EM and hadronic isolation rings are formed from the 12 towers surrounding the central cluster in the EM and hadronic layers respectively. These rings are used for isolation tests to discriminate against hadronic activity. The hadronic core energy behind the EM cluster provides additional hadronic rejection.

At the HLT, the full detector granularity is used within the ROI for the final trigger decision. Photons and electrons are identified with EM clusters, with an additional matching track requirement for electrons. The calorimeter reconstruction is typically less expensive in terms of computing, and therefore precedes the track reconstruction to reject events early. The HLT trigger sequence is shown in figure 1 (right).

3. Upgrades to Electron and Photon Identification in Run 2

In 2017 the LHC is producing collisions at greater rates and with higher than ever average pileup per bunch crossing. These conditions have prompted a number of innovative upgrades to the trigger algorithms, with the aim of reducing the trigger rate without compromising the efficiency in order to reduce and delay the need to increase trigger E_{T} thresholds. Rate predictions are

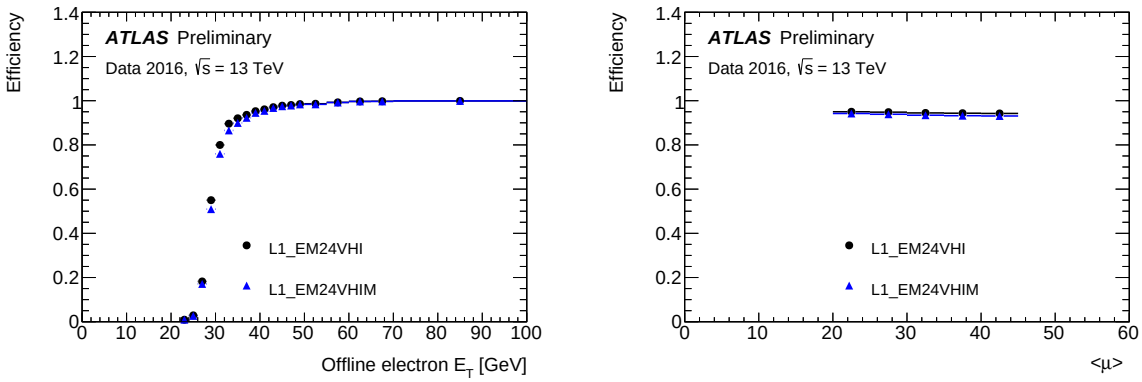

Figure 2. Performance of the new medium L1 isolation working point [9]. The efficiency is shown as a function of transverse energy (left) and the average number of interactions per bunch crossing (right). The naming convention is as follows: *L1* indicates a Level 1 trigger, *EM* indicates electromagnetic, the subsequent number indicates the transverse energy threshold, *V* indicates a pseudorapidity dependent transverse energy threshold, *H* indicates hadronic isolation and *I* indicates EM isolation. The *M* identifies the new medium working point implemented in the trigger menu for 2017 data taking.

measured using an enhanced bias dataset [5] and the electron efficiencies are measured using the *Tag and Probe* method [6] with $Z \rightarrow ee$ electrons. Photon efficiencies [7] are measured using the *bootstrap* method, where the efficiency is measured with respect to a looser L1 trigger.

3.1. L1 Reoptimisation

In 2017 the L1 isolation selection was optimised by considering variables based on the EM isolation energy compared with the cluster energy. The new 'medium' L1 isolation working point achieves a rate reduction of 10.8% with a minimal efficiency loss of 1.3% for a L1 E_{T} threshold of 24 GeV, currently the default L1 EM trigger E_{T} threshold. The medium working point is implemented for the trigger menu in 2017 data taking. The performance of the new L1 working point is shown in figure 2. The efficiency loss is mostly concentrated in the turn-on, with the plateau efficiency mostly unchanged.

3.2. Ringer Upgrade

Another Run 2 improvement to the electron trigger is the ringer upgrade to the fast calorimeter step [8]. The ringer algorithm is an alternative to the previous cut based selection which explores the conic geometry of the electron shower shape, building successive rings in the calorimeter. These are then used to build a vector of discriminating variables based on generalised shower shapes, which are fed into a neural network (NN) classifier. A Multilayer Perceptron is used with the hidden and output layer activation function set to tanh. The data is split into into a training set (60%) in which the NN weights are adjusted and a test set (40%) for verification and performance evaluation. The classifier performs particle identification targeting efficiency of the complete HLT trigger with a significant reduction to the number of calls to the inner tracking detector, which is typically more expensive in terms of computing.

The ringer algorithm achieves a $\times 2$ improved background rejection compared with the older cut based selection used in the fast calorimeter step, with the efficiency almost unchanged. The performance of the ringer trigger in 2016 is shown figure 3. The ringer algorithm is now the default in electron triggers at ATLAS.

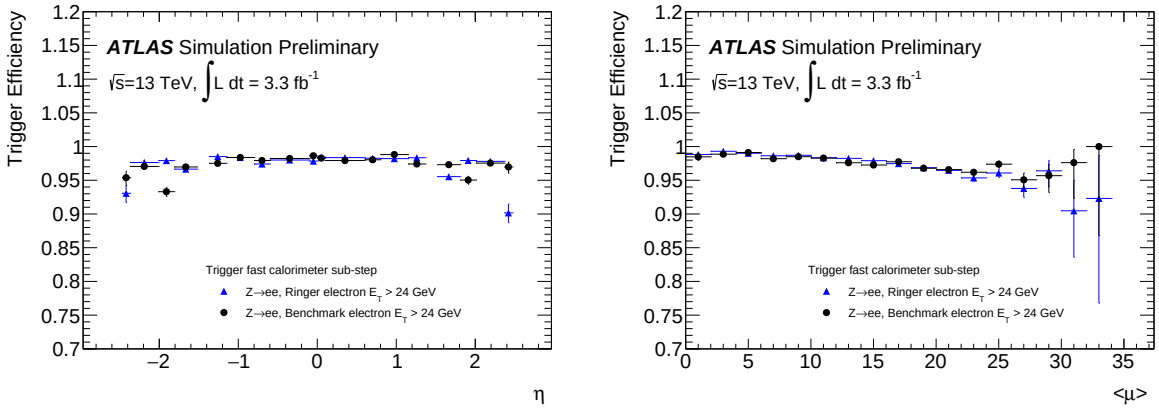

Figure 3. Performance of the ringer algorithm in the calorimeter fast-step of the HLT, compared with the previously default cut based method [9]. The efficiency is shown as a function of pseudorapidity (left) and the average pileup per bunch crossing (right).

3.3. Likelihood Based Electron Identification

A common set of variables is used for electron and photon identification [6][7]. These variables are based on properties of the EM energy cluster such as the shower shape and the energy ratios between cells within the cluster. In Run 1, cut based selections were used for both electron and photon identification, with the photon selection reoptimised in Run 2 for harsher pileup conditions, and higher instantaneous luminosity and centre-of-mass energy. In Run 2, a likelihood (LH) based approach was introduced for offline electron identification. The LH method is a multivariate analysis technique, simultaneously evaluating electron cluster variables to form a LH discriminant:

$$d_{\mathcal{L}} = \frac{\mathcal{L}_S}{\mathcal{L}_S + \mathcal{L}_B}, \qquad \mathcal{L}_{S(B)}(\vec{x}) = \prod_{i=1}^{n} P_{s(b),i}(x_i) \tag{1}$$

where $\mathcal{L}_{S(B)}$ is the signal (background) likelihood, $\vec{x}$ is a vector of the input variables and $P_{s(b),i}(x_i)$ are the signal (background) probability densities corresponding to each of the inputs. Three ID levels are formed by cutting on different values of the LH discriminant $d_{\mathcal{L}}$. These represent a tradeoff between purity and efficiency and are chosen such that the samples of electrons selected are subsets of looser IDs. The LH approach has now been introduced online, providing a better matching between online and offline identification and giving a 20% improvement in the online trigger rate for a similar efficiency. The LH identification is now the default for electron triggers in Run 2.

4. Electron and Photon Trigger Performance in 2016 and 2017

The trigger selection has been progressively tightened in Run 2 to control the trigger output rates. By tightening the identification level of the triggers the E_{T} thresholds can be maintained at a lower transverse energy than would otherwise be necessary. At L1, the trigger identification has moved from a non-isolated to an isolation based selection and the E_{T} threshold has been increased from 18 GeV at the beginning of Run 1 to 24 GeV in 2017. At HLT the likelihood based identification improved the trigger rate, and an additional 45% rate reduction was achieved in 2016 by moving from medium likelihood ID to tight likelihood ID for the single electron trigger. The single trigger E_{T} threshold has also been tightened from 24 GeV in 2015 to 28 GeV in

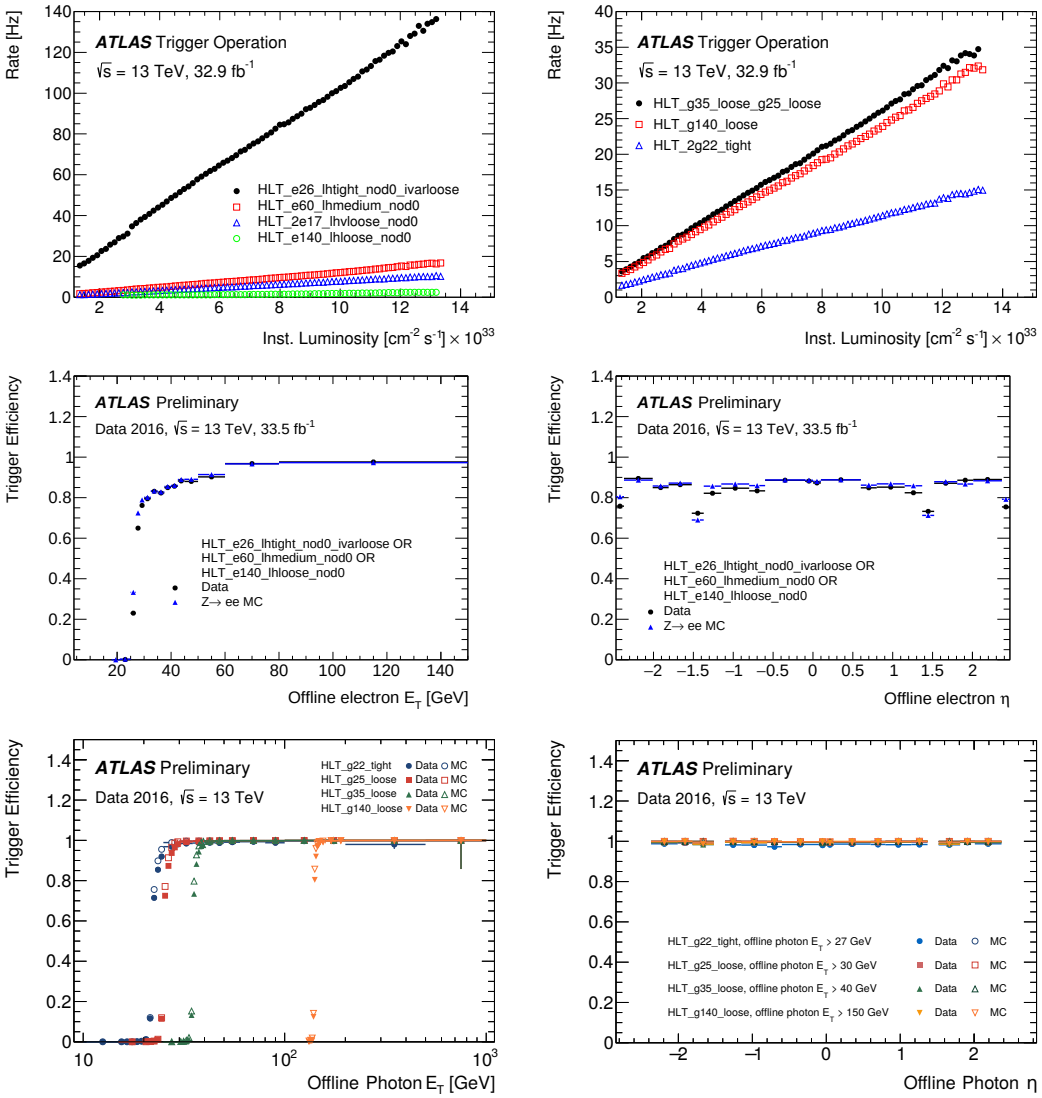

Figure 4. Trigger output rates (top) and electron (middle) and photon (bottom) performance in 2016 [9]. The efficiencies are shown as a function of transverse energy (left) and pseudorapidity (right). The electron efficiency is measured using the *Tag and Probe Method* using $Z \rightarrow ee$ decays for data and Monte Carlo. The photon efficiency is measured with the *bootstrap* method using events recorded with a looser Level 1 trigger.The naming convention is as follows: *HLT* indicates a High Level Trigger, *e (g)* indicates an electron (photon) trigger, the subsequent number indicates the transverse energy threshold, next the identification level is identified (*tight, loose* or *medium*), where *lh* is used to indicate a likelihood based trigger. *nod0* indicates that no transverse impact parameter cuts are required and *ivarloose* indicates a variable sized cone isolation requirement.

2017. For the dielectron trigger, a lower E_{T} threshold can be used. During Run 2 the dielectron trigger E_{T} threshold has been raised to 17 GeV from 12 GeV. The electron output rates for the triggers that make up the logical OR for the single electron trigger and the dielectron trigger are shown in figure 4 (top left). The electron trigger rate is dominated by $W \rightarrow e\nu$ events (around

55%), with subdominant contributions from multijet (35%) and $Z \to ee$ (10%) events.

For the photon triggers a similar strategy is employed, with the single photon E_{T} threshold progressing from 120 GeV to 140 GeV, and the 20 GeV diphoton E_{T} threshold moving to 22 GeV. For the asymmetric diphoton trigger, requiring 25 GeV and 35 GeV photons, the rate is controlled by tightening the trigger ID from a loose cut based ID to a medium cut based ID.

In 2016 and 2017 data taking variable track-isolation is used for the primary single electron trigger. At high transverse energies, track isolation losses become important. To mitigate the efficiency loss at high energies, a logical OR is used with high E_{T} threshold, looser, non-isolated triggers. The effect can be seen in the overall efficiency vs. transverse energy in figure 4 at 60 GeV where a discontinuity is seen in the trigger turn-on. A significant increase in efficiency in the plateau is achieved with minimal contribution to the electron trigger rate.

5. Conclusions

Improvements to the ATLAS e/γ triggers at L1 and HLT, particularly in rate reduction, have allowed the transition to a higher luminosity LHC without large increases from the Run 1 E_{T} thresholds and thus improving the physics potential of the experiment. The 2016 performance plots in figure 4 show excellent agreement between data and Monte Carlo simulation and a good overall performance, continuing in the most recent results for 2017 data taking. With the LHC running at design luminosity in 2018 and 2019 it is anticipated that around 80 fb^{-1} of collision data will be produced. The ATLAS e/γ triggers will continue to operate at close to the current energy thresholds, offering exciting prospects for electron and photon signatures.

References

[1] The ATLAS Collaboration 2008 *JINST* **3** S08003

[2] Evans L and Bryant P 2008 *JINST* **3** S08001

[3] The ATLAS Collaboration 2017 *Measurement of the W-boson mass in pp collisions at* $\sqrt{s} = 7$ *TeV with the ATLAS detector* `arXiv:1701.07240v1` [hep-ex]

[4] The ATLAS Collaboration 2012 *Observation of a new particle in the search for the Standard Model Higgs boson with the ATLAS detector at the LHC* `arXiv:1207.7214v2` [hep-ex]

[5] The ATLAS Collaboration 2016 *Trigger monitoring and rate predictions using Enhanced Bias data from the ATLAS Detector at the LHC* ATL-DAQ-PUB-2016-002

[6] The ATLAS Collaboration 2016 *Electron efficiency measurements with the ATLAS detector using the 2015 LHC proton-proton collision data* ATLAS-CONF-2016-024

[7] The ATLAS Collaboration *Measurements of the photon identification efficiency with the ATLAS detector using 4.9 fb1 of pp collision data collected in 2011* ATLAS-CONF-2012-123

[8] João Victor da Fonseca Pinto and ATLAS Collaboration 2016 J. Phys.: Conf. Ser. 762 012049

[9] The ATLAS Collaboration Public Egamma Trigger Plots for Collision Data `https://twiki.cern.ch/twiki/bin/view/AtlasPublic/EgammaTriggerPublicResults`